University of Szeged
Faculty of Pharmacy
Doctoral School of Pharmaceutical Sciences
Institute of Pharmaceutical Analysis

Bioanalytical Applications of LC-MS Techniques

Ph.D. thesis

Zahraa Ali

Supervisor:

Dr. Róbert Berkecz

Szeged, Hungary

2026

University of Szeged, Faculty of Pharmacy
Doctoral School of Pharmaceutical Sciences
Pharmaceutical Analysis PhD Program
Head of the program: Prof. Dr. István Ilisz, DSc.

Institute of Pharmaceutical Analysis
Supervisor
Dr. Róbert Berkecz, PhD,

Bioanalytical Applications of LC-MS Techniques

Summary of Ph.D. Thesis

Zahraa Ali

Complex Exam Committee:
Chairman
Prof. Dr. Dezső Csupor, DSc,
Members
Dr. Ágnes Dörnyei, PhD,
Dr. András Szekeres, PhD,

Defense Board:
Chairman
Prof. Dr. Dezső Csupor, DSc,
Reviewers
Dr. Ágnes Dörnyei PhD,
Dr. Zoltán Kele PhD,
Secretary
Dr. Renáta Minorics Kanizsai PhD,
Members
Dr. Gábor Kecskeméti PhD,

Szeged, Hungary
2026

Introduction

Bioanalysis is an essential branch of pharmaceutical science and an indispensable tool in drug development, drug monitoring, guided secondary metabolites discovery, and many other relevant fields. In bioanalysis, modern analytical techniques are applied to provide qualitative and quantitative information about analytes at trace concentrations. The compounds may be endogenous (Phenanthrenes) or exogenous in biological samples such as blood, plasma, urine, tissues, or plants.

Liquid chromatography coupled to mass spectrometry (LC-MS) is one of the most used techniques in bioanalytical applications due to its high sensitivity, accuracy, reproducibility, and suitability for complex biological matrices. The compounds are separated in liquid chromatography according to their retention times, providing an initial clean-up of the sample and an acceptable level of identification before they are passed to the mass spectrometry, where they are ionized, filtered, and detected as a function of their mass-to-charge ratio (m/z). Subsequently, compounds with identical retention properties can be differentiated and quantified by mass spectrometry.

When structural information is required, high-resolution mass spectrometry HRMS can provide accurate fragmentation data since it collects the exact mass with high resolution.

Nimodipine (**NMD**) is a second-generation 1,4-dihydropyridine derivative and an L-type voltage-gated calcium channel (VGCC) blocker (**Fig. 1**). It was approved by the United States Food and Drug Administration (FDA) in 1988 for the management of vasospasm following aneurysmal subarachnoid hemorrhage (aSAH). So far, **NMD** remains the cornerstone therapy for the prevention of delayed cerebral ischemia (DCI) following aSAH.

During ischemic stroke, marked tissue acidosis occurs in the brain. These pH changes are functionally important because mild acidosis reduces neuronal excitability, whereas alkalosis increases it. More importantly, marked or persistent acidosis has been recognized as a significant pathomechanism of neuronal injury. Since drug pharmacokinetics may also be influenced by pH, this factor should be considered when characterizing tissue saturation. In the present work, it is therefore essential to determine whether nimodipine, as a compound with potential neuroprotective relevance, can be effectively taken up by tissues at risk of injury under pH conditions outside the physiological range. Acute brain slice preparations are inherently devoid of cerebral circulation and provide a suitable reductionist model for investigating the direct action

of nimodipine on nervous tissue independently of its vascular effects. Since the direct effect of nimodipine on nervous tissue at risk of injury has not yet been investigated in detail, designing an acute brain slice experiment and investigating **NMD** tissue saturation kinetics can provide valuable insights, particularly under different pH conditions. Due to the complexity of brain samples, more selective and sensitive hyphenated analytical techniques are required for reliable quantitative determination of nimodipine. Tandem mass spectrometry using electrospray ionization is among the most frequently used analytical methods for **NMD** determination in animal and human samples. In particular, LC–MS/MS provides efficient chromatographic separation and sensitive, selective detection, achieving low limits of detection.

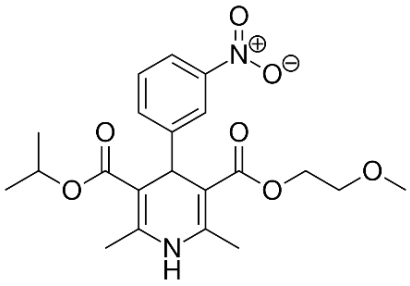

Fig. 1. Chemical structure of nimodipine

Phenanthrenes, on the other hand, are a small family of aromatic secondary metabolites naturally occurring in plants. They are found prominently in the *Orchidaceae* and *Juncaceae* families, particularly in species of the genus *Juncus.* Phenanthrenes possess a tricyclic phenanthrene skeleton, which may occur either in fully aromatic form or as 9,10-dihydrophenanthrene derivatives (**Fig.2**).

Interest in phenanthrene research has increased in recent years due to its broad range of biological activities, including antimicrobial, antioxidant, antiviral, anti-inflammatory, and cytotoxic properties, suggesting that phenanthrenes may represent promising pharmacologically relevant natural products. Particularly, phenanthrenes isolated from *J. compressus* have demonstrated notable antiproliferative activity against HeLa cervical cancer cells and considerable antiviral activity against herpes simplex virus type 2 (HSV-2). From an analytical perspective, phenanthrenes pose several challenges because they are present at trace levels in chemically complex plant extracts, and many are closely related in structure and differ only in the number or position of substituents. Moreover, the substitution pattern of phenanthrene strongly affects ionization efficiency and fragmentation behavior, which, in turn, influence both detectability and selectivity in mass spectrometric analysis. LC–MS hyphenated techniques provide an especially

suitable analytical platform for the investigation of phenanthrenes. Nevertheless, analytical studies of phenanthrene remain relatively limited compared with those of many other natural-product classes. Detailed knowledge of fragmentation behavior is especially important for phenanthrenes, as structurally similar compounds may yield related but not identical product-ion spectra. Therefore, fragmentation studies can provide valuable support for structural elucidation, analyte confirmation, distinction between closely related compounds, and the selection of suitable ions for targeted quantitative methods. Moreover, compared with positive-ion measurements, the negative-ion fragmentation behavior of phenanthrenes has been much less systematically investigated.

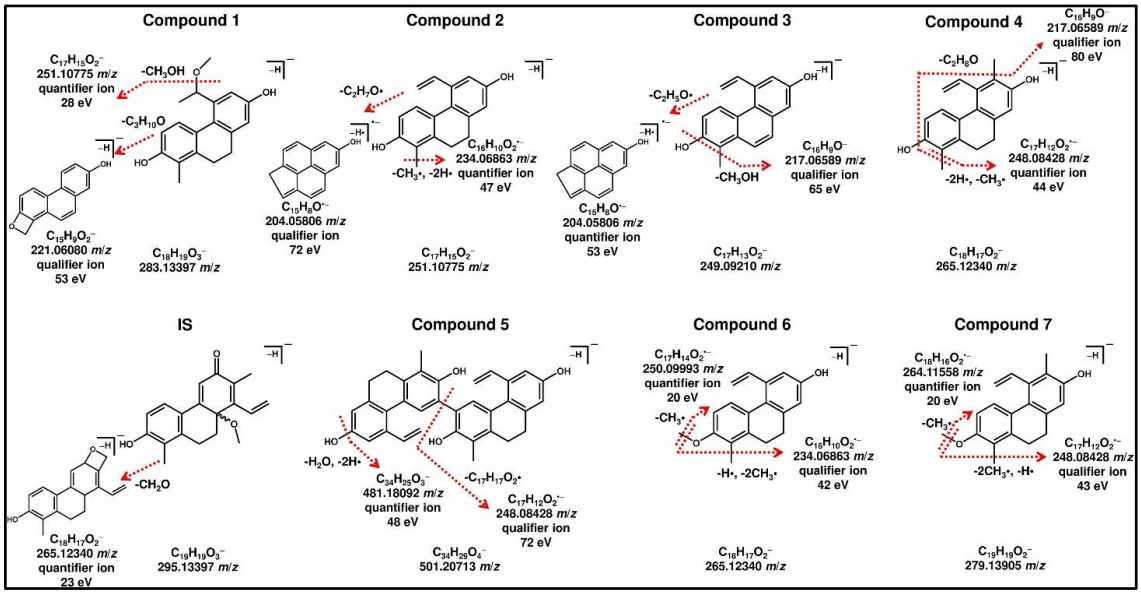

Fig. 2. Phenanthrenes structure and assumed HESI-MS/HRMS fragmentation process of investigated phenanthrenes obtaining quantifier and qualifier ions.

Aims and objectives

This work aimed to address biologically relevant questions through an analytical approach by developing, validating, and applying UHPLC-MS/MS and UHPLC-MS/HRMS methods for the qualitative and quantitative determination of targeted analytes. Novel sample preparation procedures, comprehensive fragmentation studies, state-of-the-art analytical methods, and full bioanalytical validation supported this endeavor.

Since the brain is the primary organ where **NMD** exerts its effect, and pH changes in the brain areas may influence **NMD** distribution in the CNS, we aimed to investigate the

effects of pH changes on the saturation kinetics of **NMD** in acute rat brain slice preparations. For this purpose, a targeted UHPLC-MS/MS method was developed, validated, and applied for the quantitative measurement of **NMD** levels in brain tissue using a small sample quantity and a simple liquid-liquid extraction procedure with a short chromatographic run time. In the pharmacology aspect of the new analytical method application, to the best of our knowledge, this is the first attempt to report pharmacokinetic studies of **NMD** in acute rat brain slice preparations. Another objective of our work was to address a gap in phenanthrene research by investigating its detailed fragmentation behavior in negative-ion mode, which had not been previously studied. To better understand this process, proposed fragmentation pathways were established based on MS/HRMS data. In addition, a targeted UHPLC–MS/HRMS method was developed and applied for the quantitative determination of phenanthrenes in *Juncus compressus*.

Experimental part

To investigate **NMD** saturation kinetics, acute rat brain slices were prepared from young adult Sprague-Dawley rats, and the kinetics of tissue saturation with **NMD** were characterized at three pH levels, achieved by adjusting the incubation medium. A matrix-matched external calibration method, with internal standard normalization by NMD-D7, was applied for quantitative analysis.

To enrich **NMD** and reduce the disturbing matrix effect of endogenous compounds in brain homogenate, a liquid-liquid extraction procedure was performed by spiking the brain EDTA homogenate with the internal standard solution composed of **NMD-D7** in MeOH/IPA/water (3/1/0.1 v/v/v%).

The targeted UHPLC–MS/MS analysis of **NMD** was performed using a Shimadzu Nexera (Kyoto, Japan) ultra-high-performance liquid chromatography (UHPLC) system connected via a 2-position, 6-port valve to a TSQ Fortis triple quadrupole tandem mass spectrometer (Thermo Scientific, Waltham, MA, USA). Many chromatographic columns and conditions were investigated but the final UHPLC separations were performed using a Waters Acquity UPLC BEH C18 column (2.1 mm × 50 mm, 1.7 µm particles, equipped with a guard column, Milford, MA, USA). The MS/MS analysis was performed in positive-ion multiple reaction monitoring (MRM). The final UHPLC-MS/MS method was fully validated. The UHPLC system was controlled by LabSolution Verison 5.97

SP1 (Shimadzu, Kyoto, Japan). Data acquisition, postprocessing, and quantitative evaluation of the MS/MS raw file were performed using Xcalibur 4.2 software

For Phenanthrenes analysis, dried extracts of Phenanthrenes compounds were provided by the Department of Pharmacognosy, University of Szeged, and extracts (n = 3) were prepared from the aerial parts of J. compressus collected during the flowering period in Hungary.

The MS/HRMS and UHPLC-MS/HRMS measurements of phenanthrenes were performed by Waters Acquity I-Class UPLC (Milford, MA, USA) and Thermo Scientific Q Exactive Plus Hybrid Quadrupole-Orbitrap (Waltham, MA, USA) mass spectrometer. The mass spectrometer was equipped with heated electrospray ionization (HESI) mode. The MS/HRMS analysis was performed in negative-ion scheduled parallel reaction monitoring (PRM). Several columns were studied for method development, but for the final UHPLC separation of phenanthrenes, the Accucore C30 column (150 × 2.1 mm, 2.6 μm) with an Accucore C30 guard column (10 × 2.1 mm, 2.6 μm) from Thermo Fisher Scientific (Waltham, MA, USA) was selected. The final quantitative analysis was carried out in one batch, using an external calibration approach and the final method was validated. For controlling the UHPLC instrument, MassLynx 4.1 (Milford, MA, USA) software was used, while the HRMS data acquisition occurred by Xcalibur 4.4 software (Waltham, MA, USA). For quantitative evaluation of the UHPLC-MS/HRMS data, the raw files were processed using the Xcalibur software. The one-way ANOVA statistical analysis followed by Bonferroni's post hoc test was performed by GraphPad Prism 5.0 (GraphPad Software, San Diego, CA, USA) software.

Bond dissociation energies (BDEs) obtained from quantum-chemical calculations were used to determine the initial steps of the fragmentation pathways of the investigated compounds, yielding the observed distribution.

Results

I. A high-throughput UHPLC-MS/MS method was developed for the selective and sensitive quantitation of NMD in acute rat brain tissue using a low amount of brain homogenate.

A novel UHPLC-MS/MS method was successfully developed in this thesis to provide a highly sensitive and selective analytical approach for determining **NMD** trace concentrations in the brain. Given the scarcity of UHPLC-MS/MS methods for **NMD** at its site of action, it is highly relevant to develop a robust, reproducible, and fast analytical method to investigate brain tissue saturation with **NMD**.

The fragmentation behavior of **NMD** was thoroughly studied, beginning with the determination of suitable mass spectrometry conditions. **NMD** showed favored detection in positive ionization mode. The flow injection method was chosen over the direct infusion method because the protonated form ([**NMD**+H]$^+$) in positive mode was predominant over the sodium adduct of **NMD** ([**NMD**+Na]+) formed by direct infusion. The deuterium-labeled **NMD** (**NMD-D7**) was used to eliminate or minimize signal variability (resulting from sample preparation, LC injection, spray stability, etc.) and was selected as an internal standard for quantitative analysis.

For targeted UHPLC-MS/MS analysis, two transitions per compound were selected for quantitative analysis and qualitative confirmation within a related retention time window. The study of the fragmentation behavior of single-charged protonated **NMD** molecular ion [M+H]$^+$ at 419.2 *m/z* resulted in the production of two main fragment ions (**Fig.3**) at 343.1 *m/z* and 301.1 *m/z* as the quantifier (for quantitation) and qualifier ion (for confirmation). For **NMD-D7**, 426.2 *m/z* –350.2 *m/z* and 426.2 *m/z* –302.1 *m/z* transitions were selected, and the corresponding CEs were optimized. The most abundant fragment ion, the quantifier ion, was produced by losing the 2-methoxyethyl group from the ester at the fifth position, yielding a resonance-stabilized acylium ion, and its resonance structures are shown in **Fig. 4** for both **NMD** and **NMD-D7**. For the qualifier ion, a further fragmentation process forms a free carboxyl group at the third carbon atom via cleavage of the ester bond.

The application of the BEH C18 column provided a symmetrical and narrow (<0.08 min) chromatographic peak for **NMD**, applying 0.1% FA in water as an A eluent and 0.1% FA in ACN as a B eluent. Studying the contribution of organic solvents to chromatographic and mass spectrometric parameters of **NMD**, higher retention (2.74

min) and higher pressure were observed with MeOH compared with ACN, as expected. To avoid retention of brain lipids in the column during the gradient program wash, ACN with a higher eluent strength than MeOH was selected as the organic solvent for the B eluent. The increased FA content in the mobile phase from 0.1% to 1% did not result in significant changes in peak retention time or peak area for both ACN and MeOH, indicating that the protonated form of **NMD** is dominant over this FA concentration range. The purpose of the gradient program optimization was to achieve satisfactory peak width, peak symmetry, and retention for **NMD** within a 5-minute total run time, comparable to or better than earlier published LC methods for quantifying **NMD** in biological samples. The application of a flow rate of 0.4 mL/min, a column temperature of 50 °C, and a linear gradient assisted in keeping the required chromatographic parameters. The application of the final UHPLC-MS/MS method yielded a symmetrical peak shape for **NMD** with a retention time of 2.35 min (**Fig.4**). The application of toluene resulted in a high recovery of **NMD** in brain homogenate, accompanied by negligible matrix effects due to the more selective enrichment of **NMD** relative to coeluting brain endogenous compounds, such as brain phospholipids. The two MS/MS transitions of **NMD** and **NMD-D7**, along with their ratios, were also monitored to exclude the apparent isobaric effect. The quantifier-to-qualifier ion ratios were 2.3 for **NMD** and 2.5 for **NMD-D7** in the analysis of brain samples. Moreover, our analytical method requires only 20 µL of brain homogenate, having a 0.091 mg brain/µL homogenate concentration. The stability of **NMD** for 3 days without any degradation was obtained in brain homogenate with the use of 5 mM EDTA solution at a pH of 5.5. Regarding the low solubility (2.3 µg/mL) and instability of **NMD** in an aqueous solution, the MeOH/IPA/water (3/1/0.1, V/V/V) mixture was selected for dissolving the dry extract, forming a stable homogenous solution without significant influence on chromatographic retention and peak shape of **NMD**.

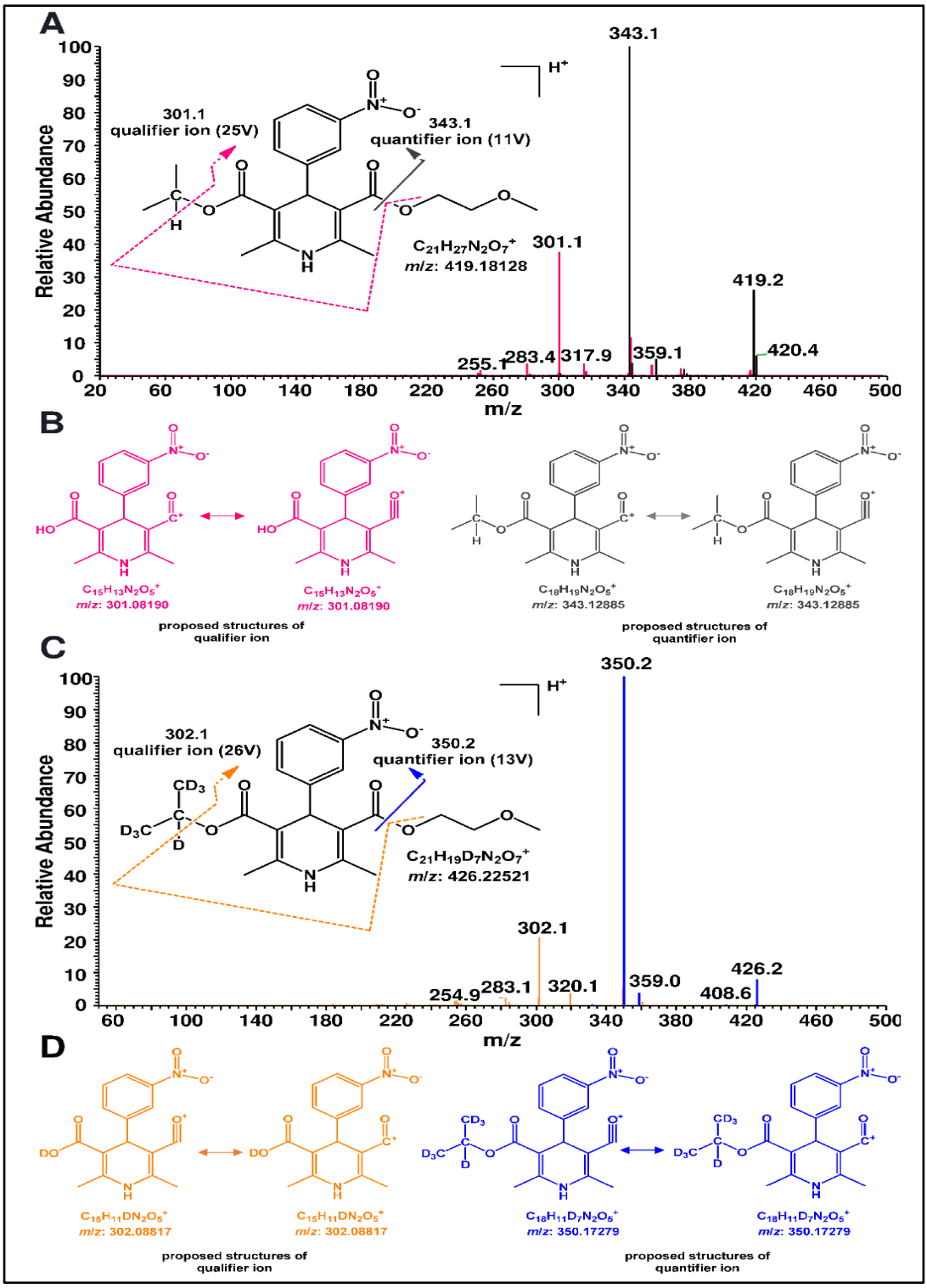

Fig. 3. (A) Overlayed MS/MS spectrum of **NMD** at optimized CE. (B) Proposed structure of quantifier (magenta) and qualifier ions (gray) of **NMD**. (C) Overlayed MS/MS spectrum of **NMD-D7** at optimized CE. (D) Proposed structure of quantifier (magenta) and qualifier ions (gray) of **NMD-D7**.

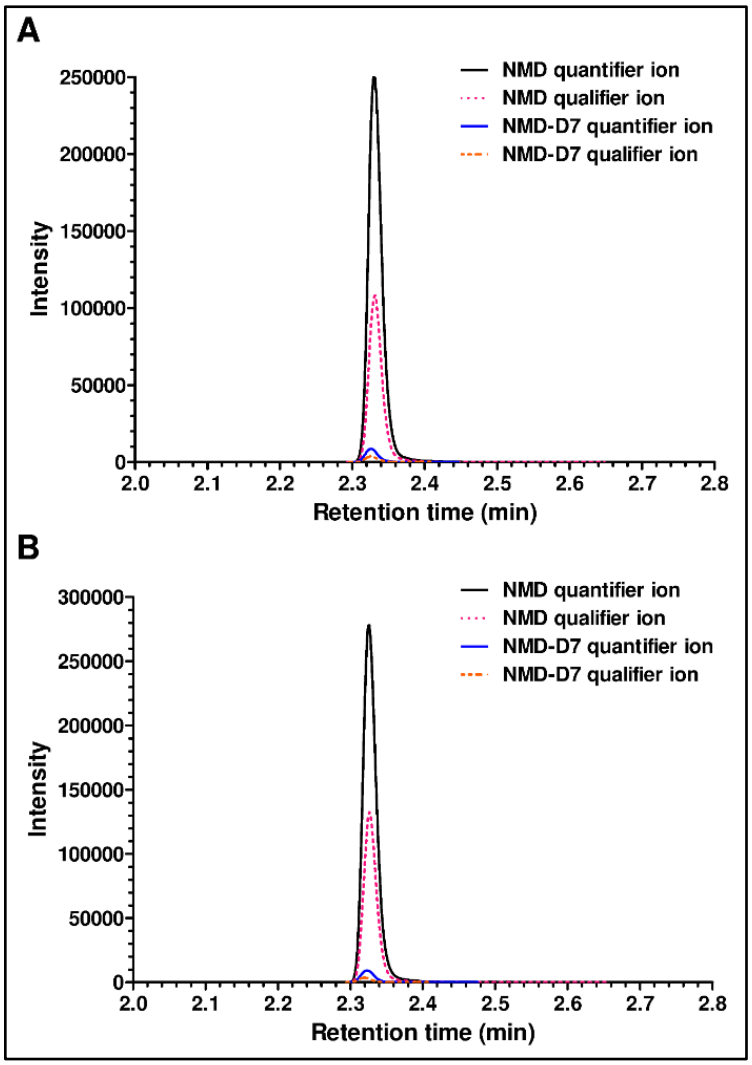

Fig. 4. (A) Extracted ion chromatogram of concentration calibration point (22.924 µg/g): **NMD** quantifier ion (black straight line), **NMD** qualifier ion (magenta dashed line), **NMD-D7** quantifier ion (blue straight line), **NMD-D7** qualifier ion (orange dashed line). (B) Extracted ion chromatogram of *in vitro* sample (pH: 7.38 , *in vitro* treatment time: 30 min): **NMD** quantifier ion (black straight line), **NMD** qualifier ion (magenta dashed line), **NMD-D7** quantifier ion (blue straight line), **NMD-D7** qualifier ion (orange dashed line).

II. The developed targeted UHPLC–MS/MS method was validated

One of the gaps in **NMD** research is the lack of a fully validated UHPLC-MS/MS method capable of detecting **NMD** at trace levels in the brain, and that is reproducible for further applications.

In this work, the newly developed UHPLC-MS/MS method was fully validated, and the applied validation criteria were determined in accordance with the ICH guideline for the validation of analytical procedures Q2(R1). The calculated and practical LLOD was determined to be 15 ng/g brain (547 fg injected **NMD** into the column) and was lower than previously reported (30 and 50 ng/g brain). The study of calibration curve type and weighting showed that a linear approach without weighting yielded the best fit. For the linearity of the calibration curve across five independent calibration series, the concentration range was 0.023-229.2 µg/g brain, and the coefficient of determination (R2) was greater than 0.99. The calibration curve spanned a wider concentration range than earlier published methods (0.05-20 µg/g brain). The obtained bias values fell within the accepted ±20% for LOW and ±15% for MID and HIGH concentration levels, respectively. The within-run and between-run precision values were below 5 and 10.5% in the coefficient of variation (CV). With the high enrichment of **NMD** in the organic toluene phase, the recovery of **NMD** was 96.9–110.6%, higher than previously reported. The negative matrix effect (less than 10% of ion suppression) was observed only at the MID concentration level, while it was positive (3.3–12.9% of ion enhancement) for other levels, which indicates the ability of the developed sample preparation procedure to effectively eliminate the endogenous compounds disturbing the ionization of **NMD** from complex brain homogenate. The process efficiency, as a resultant of the recovery and matrix effect values, was in the range of 100.6–109.4%. To obtain valid analytical results, the stability of the targeted compound is an important aspect in tissues, homogenates, and prepared samples. The revealed stability values of **NMD** suggested that no significant analyte loss took place in any of the quality control (QC) samples, suggesting that samples awaiting analysis are stable for up to 3 days in brain homogenate (at 4 °C), one day in the extract form (at 16 °C), one year in tissue (at −80 °C), and after three freeze–thaw cycles. The calculated mean carry-over of **NMD**, determined from **NMD**-free brain samples measured after the highest calibration points, was also negligible (0.07%). Over hundreds of validation runs, no retention time shifting was observed, and the **NMD** retention time was 2.35 ± 0.1 min. The selectivity study confirmed that no

significant response attributable to interfering components was observed at the retention time of **NMD** and **NMD-D7** in the blank samples.

III. The developed UHPLC-MS/MS method was applied in the determination of the *in vitro* pharmacokinetic curve of NMD in acute rat brain slices

The kinetics of tissue saturation with **NMD** were characterized at three pH levels, achieved by adjusting the incubation medium with 1 M HCl or 1 M NaOH. The three conditions established were physiological (pH 7.38), acidic (pH 6.50), and alkaline (pH 7.57).

The measured concentration of **NMD** in the brain slice treated for 0.5 min and then rinsed with PBS solution is, according to our assumption, the result of surface adsorption processes. No significant changes were found in adsorbed **NMD** compared to the three pH assays at a 95% confidence level, and the mean concentrations of **NMD** were below 5.5 µg/g brain in each case (**Fig. 5**). The saturation of brain tissues with **NMD** occurs uniformly in 50 min (t_{max}) to reach median **NMD** concentrations of 31.93 (pH 7.38), 46.16 (pH 6.50), and 30.89 µg/g (pH 7.57). Based on the above data, approximately 14% of the total **NMD** content can be assigned to surface binding. This relatively high value might be explained by the strong hydrophobic interaction between the lipophilic **NMD** and the lipid-rich brain tissue. By studying the effect of the brain tissue pH on **NMD** absorption, no significant differences were found in the analysis of variance (ANOVA) analysis conducted to compare the experimental conditions in the time range of 50–60 min. During the time-dependent examination of **NMD** concentrations during a given pH treatment, no significant differences were found in any experimental arrangements when analyzing the concentrations obtained at 50 and 60 min, as shown in **Fig. 7**. It can be summarized that at all three pH values, the plateau of the kinetic curve is located in the 50–60 min time interval. The statistical analysis of the obtained concentrations confirmed that no chemical degradation of **NMD** was observed as the treatment time progressed.

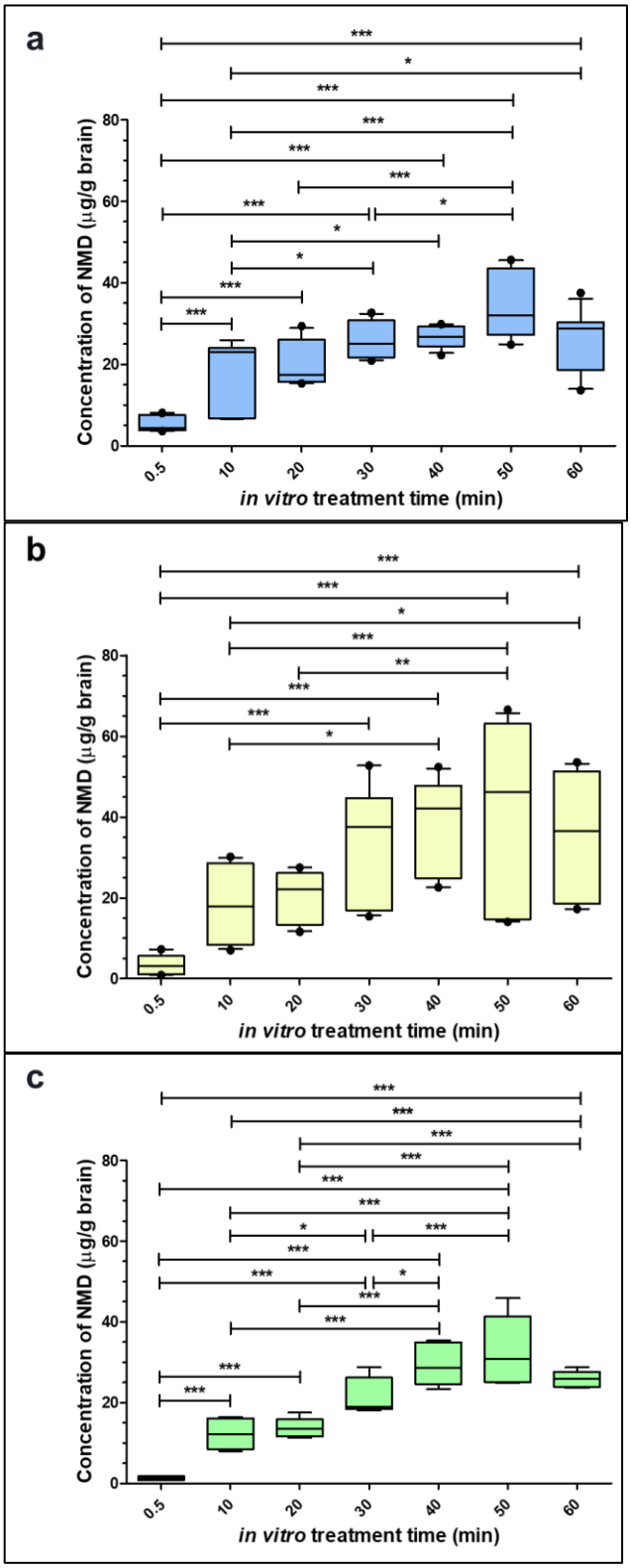

Fig. 5. (A) Pharmacokinetic curve of **NMD** in brain slices (pH: 7.37, n = 3). (B) Pharmacokinetic curve of **NMD** in brain slices (pH: 6.50, n = 3). (C) Pharmacokinetic curve of **NMD** in the brain.

IV. The negative-ion MS/HRMS fragmentation behavior of phenanthrenes was characterized and identified a novel "organ pipe distribution" phenomenon, supported by quantum chemical calculations.

Despite the pharmacological and phytochemical relevance of phenanthrenes, their analytical investigation remains relatively limited. Broader mass spectrometric characterization of phenanthrenes remains insufficient, particularly for interpreting their fragmentation pathways.

In our study, the fragmentation behavior of phenanthrenes (**Fig. 6**) was investigated based on their predicted chemical compositions derived from MS/HRMS spectra. They showed better ionization efficiency in the negative mode due to the presence of the phenolic hydroxy group(s) and the lack of a relatively easily protonable functional group. Therefore, the negative HESI mode was selected to characterize phenanthrenes by direct infusion with HRMS and MS/HRMS. In the proposed structures of the most abundant fragment ions, the negative charge was assumed to be localized on the phenolate group, supporting the formation of stable phenolate-type ions in negative ionization mode. Moreover, the MS/HRMS data revealed that the given precursor ions (**Compounds 2–4, 6**) and the formed fragment ions (**Compounds 1–7**) provided special fragmentation behavior like "organ pipe distributions". As the collision energy (CE) increased, new fragment-ion peaks emerged within a 1–9 Da mass range relative to the isolated precursor ion, and adjacent ions differed by 1 Da. The shape of this distribution changed continuously as CE increased. This can be explained by the serial loss of the hydrogen radical (H•), which still resulted in fragment ions with a single negative charge. A stepwise quantum chemical approach was applied to identify the most probable bonds and fragmentation routes responsible for this behavior. The quantum-chemical results supported the proposed mechanism for this special fragmentation behavior.

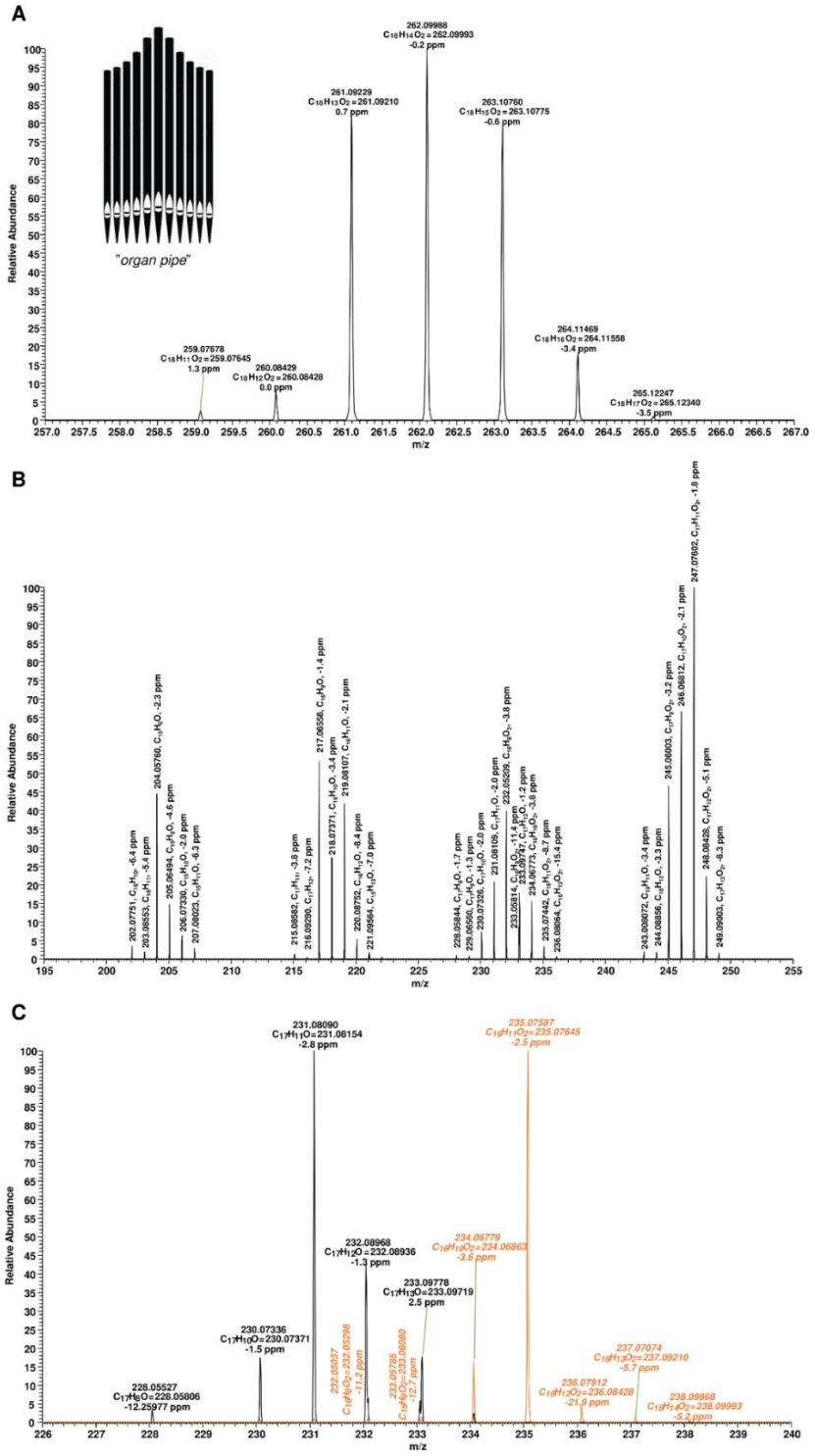

Fig. 6. The "*organ pipe distribution*" of precursor ion (A), fragment ions (B), and overlapped fragment ions (C) of **Compound 4** with related molecular compositions and mass accuracies, obtained by direct infusion HESI-MS/HRMS measurement at 49 (A), 70 (B), 36 (C orange), and 85 (C black) eV labeling molecular composition and mass accuracy

V. A new UHPLC-MS/HRMS method was developed for the analysis of phenanthrenes in *J.compressus* extracts

Phenanthrenes pose many analytical challenges, and only a handful of studies have employed LC–MS or LC–MS/MS methods for their determination. The available reports differ considerably in chromatographic mode, ionization polarity, and mass spectrometric strategy. We developed a novel UHPLC-MS/HRMS method for the quantitation of phenanthrene compounds in *J. Compressus* extracts.

By setting the initial UHPLC conditions, the HESI source was optimized for phenanthrenes using a flow-injection procedure with a T-mixer. For the HESI-MS/HRMS detection of phenanthrenes, the quantifier ions were monitored during method development. Relative to the 100-mm-length column, the highest retentions were observed on the HSS T3 column, while the use of Kinetex Biphenyl provided the lowest retention times. **Compounds 7** and **6** eluted with the highest retention times, probably due to the presence of a single phenolic hydroxyl group compared with other phenanthrenes having 2 or 4 aromatic hydroxy groups. For instance, even for **Compound 5**, a dimer of **Compound 2** containing six rings, lower retention times were observed than for **Compounds 7** and **6**, highlighting the importance of phenolic hydroxyl groups for the retention mechanism. For **Compound 1**, the presence of a 1-methoxyethyl group instead of a vinyl group at C-5 afforded the lowest retention. Steric hindrance between the analyte and the solid phase may have triggered this observation. Baseline separation was achieved for all phenanthrenes except for **Compounds 2** and **3**, which differed in only one double bond. To obtain better chromatographic parameters, Accucore C30 was selected for further chromatographic optimization. By a slight modification to the gradient program, baseline separation within 4 min was achieved for the targeted phenanthrenes, except for **Compounds 2** and **3**. The internal standard semisynthetic phenanthrene (IS) eluted in the middle of the analysis time (tR = 3 min).

VI. The targeted phenanthrenes were quantified in *Juncus compressus* by the new UHPLC-MS/HRMS method

As an application of the developed UHPLC-MS/HRMS method, all seven phenanthrene compounds were quantified in *J. compressus*. The fragment ions were PRM-monitored for each standard in the 1.5–5 min time range. Using this semi-targeted approach, five new isomers were identified: I-1, I-2 (isomers of Compound 3), I-3 (an isomer of Compound 6 or Compound 4), and I-4 and I-5 (isomers of Compound 5). According to the obtained MS/HRMS spectra of new isomers (**Fig. 7**), the precursor ions I-1, I-2, and I-3 showed the "organ pipe distribution" and a lack of 15 Da loss indicated the presence of two phenolic groups. The comparison of MS/HRMS spectra of I-3, **Compound 4** (two phenolic groups), and **Compound 6** (one phenolic group) reveals the structural similarity between I-3 and **Compound 4**. The fragmentation patterns of I-4 and I-5 were found to be in agreement with Compound 5, suggesting the existence of free phenolic groups. Given the wide concentration range of the targeted phenanthrenes, a dilution series was used to quantify them. The minor components, Compounds 1, 6, and 7, were quantified in the 0.1 mg/mL dry extract (MeOH) samples, while the concentrations of Compounds 2 and 3 were determined in samples diluted tenfold and hundredfold, respectively. The comparison of the phenanthrene concentration (nmol g-1) in MeOH and CH_2Cl_2 extracts affirmed that the latter provided higher enrichment for **Compounds 1-5**. However, **Compounds 6 and 7,** which contain a methylether group instead of a phenolic hydroxyl group, exhibited higher enrichment in the MeOH phase, likely due to their better solubility in the polar protic organic solvent. Additionally, no significant differences in concentration normalized to plant dry weight were observed between the two extracts, except when the phenanthrene content of the MeOH extract was close to or below the detection limit. **Compound 2** was detected at the highest concentration in the plants, particularly in Plants 1 and 3, with values exceeding 2300 nmol g-1. This value is significantly higher than those in Plants 2, 4, and 5. **Compound 3** was the second-most abundant (~1000 nmol/g) phenanthrene in Plants 1 and 3, which, again, is a significant difference compared with the other Plants. Considering the other examples of the concentration scale, **Compound 1** was quantified in the undiluted CH_2Cl_2 extracts of Plants 1, 3, and 5 at 4.15, 4.73, and 3.10 nmol/g.

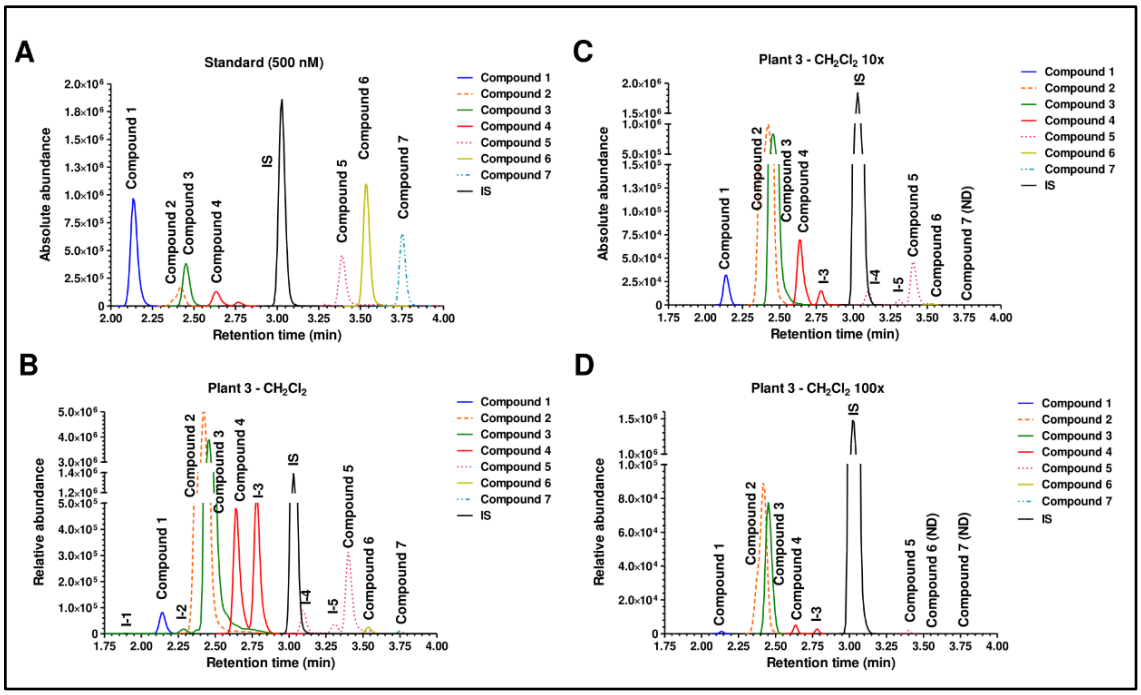

Fig. 7. Extracted ion chromatogram of targeted phenanthrenes and their isomers in (A) 500 nM calibration sample, (B) 0.1 mg/mL CH_2Cl_2 fraction from Plant 3, (C) tenfold- and (D) hundredfold-diluted CH_2Cl_2 fraction of Plant 3 obtained by UHPLC–MS/HRMS method.

Summary

Two analytical methods were developed, validated, and applied in the framework of this thesis. In case of **NMD**, a novel UHPLC-MS/MS method was successfully developed, validated, and applied to monitor **NMD** saturation in *in vitro* brain tissue samples. The pharmacokinetic profile indicates that brain tissue saturation with **NMD** occurs within 50 min at 10 µM, independent of pH. **NMD** levels remained stable between 50–60 min across three different pH conditions, while the *in vitro* model also revealed notable adsorption of lipophilic **NMD** to lipid-rich brain tissue.

For phenanthrene, the structural background underlying its distinctive fragmentation behavior, "organ pipe distribution", was elucidated. Moreover, the newly developed UHPLC–MS/HRMS method enabled the identification of additional phenanthrene isomers. Considering the high concentration range of the targeted phenanthrenes, the dilution series approach was successfully applied for their quantitation in methanolic and CH_2Cl_2 extracts. Based on ANOVA evaluation of the quantitative data, three distinct groups with similar phenanthrene profiles were identified—Plants 1–3, Plants 2–4, and Plant 5—reflecting their geographical location.

Publications related to the subject of the thesis

This thesis is based on the following publications:

I. **Ali, Z.,** Frank, R., Körmöczi, T., Ilisz, I., Domoki, F., Weicznere, R., Bari, F., Farkas, E., Berkecz, R., (2024). UHPLC-MS/MS approach for following nimodipine saturation kinetics in acute rat brain slice. **Journal of analysis and testing** 8, 466–477 *https://doi.org/10.1007/s41664-024-00316-z*

IF 7.0 (D1)

II. Körmöczi, T., Barta, A., Bogár, F., **Ali, Z**., Bús, C., Hohmann, J., Domoki, F., Ilisz, I., Weiczner, R., Vasas, A., & Berkecz, R. (2025). Study of phenanthrenes from their unique mass spectrometric behavior through quantum chemical calculations to liquid chromatographic quantitation. **Talanta**, 281, 126799. *https://doi.org/https://doi.org/10.1016/j.talanta.2024.126799*

IF 6.1 (Q1)

Accumulative IF: 13.1

Publications not related to the thesis

I. Shao, Y., Chang, C., Huang, G., Yang, X., Hu, E., Ru, Y., **Ali, Z.**, Koch, M.A., Dernovics, M., Zhang, H. (2026) Critical review on the selenium speciation data reported for the Se-accumulator plant Cardamine violifolia/hupingshanensis /enshiensis: time to move beyond the myth of abundant selenocysteine/selenocystine content. **TrAC Trends in Analytical Chemistry**, in press

IF 12.0 (D1)

II. **Ali, Z.,** Lőrinczi, B., Simon, P., Cs. Fazakas, Cs., Wilhelm, I., Bogar, F., Ilisz, I., Vécsei, L., Szatmári, I., Berkecz**,** R., (2026) A comprehensive analytical approach for investigating the enhanced *in vitro* blood–brain barrier permeability of new kynurenic acid derivatives (**Talana**, under review)